General Disclaimer

One or more of the Following Statements may affect this Document

- This document has been reproduced from the best copy furnished by the organizational source. It is being released in the interest of making available as much information as possible.

- This document may contain data, which exceeds the sheet parameters. It was furnished in this condition by the organizational source and is the best copy available.

- This document may contain tone-on-tone or color graphs, charts and/or pictures, which have been reproduced in black and white.

- This document is paginated as submitted by the original source.

- Portions of this document are not fully legible due to the historical nature of some of the material. However, it is the best reproduction available from the original submission.

Produced by the NASA Center for Aerospace Information (CASI)

NASA TECHNICAL MEMORANDUM

NASA TM X-73378

(NASA-TM-X-73378) TECHNIQUES OF GLOBAL ANALYSIS APPLIED TO GRAVITATION THEORIES: A COSMOLOGICAL BLACK HOLE? (NASA) 19 p HC A02/MF A01 CSCL 03B

N77-22029

Unclas

G3/90 24448

TECHNIQUES OF GLOBAL ANALYSIS APPLIED TO GRAVITATION THEORIES: A COSMOLOGICAL BLACK HOLE?

By George Debney
Space Sciences Laboratory

February 1977

APR 1977
RECEIVED
NASA STI FACILITY
INPUT BRANCH

NASA

George C. Marshall Space Flight Center
Marshall Space Flight Center, Alabama

TECHNICAL REPORT STANDARD TITLE PAGE

1. REPORT NO. NASA TM X-73378	2. GOVERNMENT ACCESSION NO.	3. RECIPIENT'S CATALOG NO.
4. TITLE AND SUBTITLE Techniques of Global Analysis Applied to Gravitation Theories: A Cosmological Black Hole?		5. REPORT DATE February 1977
		6. PERFORMING ORGANIZATION CODE
7. AUTHOR(S) George Debney*		8. PERFORMING ORGANIZATION REPORT #
9. PERFORMING ORGANIZATION NAME AND ADDRESS George C. Marshall Space Flight Center Marshall Space Flight Center, Alabama 35812		10. WORK UNIT NO.
		11. CONTRACT OR GRANT NO.
12. SPONSORING AGENCY NAME AND ADDRESS National Aeronautics and Space Administration Washington, D.C. 20546		13. TYPE OF REPORT & PERIOD COVERED Technical Memorandum
		14. SPONSORING AGENCY CODE

15. SUPPLEMENTARY NOTES

Prepared by Space Sciences Laboratory, Science and Engineering

*Permanent Address: Virginia Polytechnic Institute and State University, Blacksburg, Virginia

16. ABSTRACT

An elementary model of freely falling observers and emitters within a black hole's radius is examined to determine the redshift spectrum reaching a typical observer. The model is independent of scale, the fundamental unit being the radius (mass) of the black hole. The observers/emitters all follow the same kinds of trajectories: radially inward and starting from rest at spatial infinity. The "test-particle" role is assumed throughout; i.e., the observers/emitters do not themselves contribute to the gravitational field of the system. By means of redshift formulas and luminosity distance to the emitters, a picture of actual redshifts and blueshifts, with their intensities, emerges for an observer within the black hole's radius. No luminosity distances greater than approximately one-half the radius are considered in this particular study; nevertheless, redshifts and blueshifts up to approximately 0.6 are seen in portions of the observer's celestial sphere (i.e., his sky). An exotic application can be made, as a curiosity, to a black hole the size of the universe, resulting in a particular anisotropic "cosmology."

17. KEY WORDS	18. DISTRIBUTION STATEMENT Unclassified — Unlimited Wesley Darbro

19. SECURITY CLASSIF. (of this report)	20. SECURITY CLASSIF. (of this page)	21. NO. OF PAGES	22. PRICE
Unclassified	Unclassified	19	NTIS

MSFC - Form 3292 (Rev December 1972)

For sale by National Technical Information Service, Springfield, Virginia 22151

TABLE OF CONTENTS

	Page
INTRODUCTION	1
ANALYTICAL PRELIMINARIES	1
LUMINOSITY DISTANCE	6
NUMERICAL RESULTS	9
DISCUSSION	9
AN EXOTIC APPLICATION: COSMOLOGICAL SCALING	14
REFERENCES	15

TECHNICAL MEMORANDUM X-73378

TECHNIQUES OF GLOBAL ANALYSIS APPLIED TO GRAVITATION THEORIES: A COSMOLOGICAL BLACK HOLE?

INTRODUCTION

In the past several years a great number of theoretical studies of black holes have appeared in the literature. Astrophysical applications have involved, for the most part, models where the observer is placed far away from one of these collapsed objects. Although there is apparently a lower limit to the mass of an existing black hole formed in the "big bang" [1,2], it is not clear what a reasonable upper limit might be. Models of collapsed stars and collapsed galaxies seem to have received, however, the greatest attention.

The investigation considered here takes a different (albeit elementary) approach to a black-hole phenomenon. One first excludes from the context any requirement that there be far-away static observers or emitters of photons and replaces it with the requirement that all emitters and observers are falling radially inward, through the horizon surface at $r = 2$ m, and toward the singularity at the center where $r = 0$. Instead of using the typical Friedmann model for a collapsing dust, it is assumed that the masses of the infalling particles are negligible and that these are all test particles in the local Schwarzschild geometry.

The primary results of this study are manifested in the pattern and intensity of redshifted objects in the sky of a typical observer who has fallen into the black hole. None of these results depend upon the mass of the black hole, although the mass determines the scale of the whole model. To date no results have been computed for emitters which are placed at greater distances than $r = 4$ m.

ANALYTICAL PRELIMINARIES

Consider a spherically symmetric collapsed mass around which a horizon at $r = 2$ m has formed and restrict the future to contain only noninteracting test particles. Suppose all families of test particles are falling radially inward

toward $r = 0$, having started from rest at $r = \infty$. This gives rise to a geometry which is the standard Schwarzschild metric filled with test particles and dominated by the mass $\underline{m}$ of the black hole. (The uniform boundary condition at $r = \infty$ merely sets up an "average" case to analyze.)

The most convenient form in which to express the geometry here is that of the Eddington-Finkelstein ingoing Schwarzschild metric:

$$ds^2 = g_{\mu\nu} dx^\mu dx^\nu = dr^2 + r^2 (d\theta^2 + \sin^2\theta \, d\phi^2) - d\bar{t}^{\,2} + \frac{2m}{r} (dr + d\bar{t})^2 \quad , \tag{1}$$

where $\bar{t} \equiv t + 2m \cdot \ln|(r/2m) - 1|$ and t is the standard time for a faraway static observer. Removing the factor of $2m$ eliminates the mass dependence of the scale so that coordinates, R, T defined by $2mR \equiv r$, $2mT \equiv \bar{t}$, and $2mS = s$ can be utilized. Hence, equation (1) reduces to

$$(2m)^{-2} ds^2 = dS^2 = dR^2 + R^2 (d\theta^2 + \sin^2\theta \, d\phi^2) - dT^2 + \frac{1}{R} (dR + dT)^2 \quad . \tag{2}$$

The horizon surface of the black hole now lies at $R = 1$.

Any curve or trajectory in this space uses the fundamental form [equation (2)] to compute the length of its tangent vector. For the null (photon) trajectories the "length" is zero. Such a curve would possess $[R(\nu), \theta(\nu), \phi(\nu), T(\nu)]$ as its formula, where ν is a parameter along the curve. In this latter case the tangent vector $\vec{K} \equiv (\dot{R}, \dot{\theta}, \dot{\phi}, \dot{T})$ would obey:

$$0 = \dot{R}^2 + R^2 (\dot{\theta}^2 + \sin^2\theta \, \dot{\phi}^2) - \dot{T}^2 + \frac{1}{R} (\dot{R} + \dot{T})^2 \quad , \tag{3}$$

where $d/d\nu \equiv$ "dot." For non-null trajectories one simply uses $\underline{S}$ as the parameter so that the curve is given through $[R(S), \theta(S), \phi(S), T(S)]$ and its tangent vector obtained by taking d/dS. The analogous result to equation (3) is then:

$$\pm 1 = \left(\frac{dR}{dS}\right)^2 + R^2\left[\left(\frac{d\theta}{dS}\right)^2 + \sin^2\theta\left(\frac{d\phi}{dS}\right)^2\right] - \left(\frac{dT}{dS}\right)^2 + \frac{1}{R}\left[\frac{dR}{dS} + \frac{dT}{dS}\right]^2 , \tag{4}$$

where ± 1 indicates the spacelike or timelike nature, respectively, of the curve under consideration. Particles going less than the speed of light are timelike.

A feature of the Schwarzschild metric is that null trajectories, no matter what their individual properties, fall into two classes. This is most easily demonstrated by taking $\dot{\theta} = \dot{\phi} = 0$ in equation (3) to produce radial photon trajectories. In this case one obtains two tangent vectors, $\vec{K}_{IN}$ and $\vec{K}_{OUT}$, at each point (R, θ, ϕ, T) in the space; i.e., assuming $\vec{K}$ is future-pointing $(\dot{T} > 0)$ produces:

$$\vec{K}_{IN} = (-1, 0, 0, 1) ; \quad \vec{K}_{OUT} = \left(-1, 0, 0, \frac{1+R}{1-R}\right) . \tag{5}$$

Notice that if $R > 1$, then $\vec{K}_{IN}$ points "inward" and $\vec{K}_{OUT}$ points "outward" on a simple R-T coordinate graph. If $R < 1$, then both vectors point "inward" but the names of the classes still persist. If $R = 1$, a limiting process must be used since equation (5) would be invalid for $\vec{K}_{OUT}$. In this case $\vec{K}_{OUT} = (0, 0, 0, 1)$, whereas $\vec{K}_{IN}$ is the same throughout. These two classes exist at each point of the space for the other directions when $\dot{\theta}$ or $\dot{\phi}$ is not zero, but are somewhat harder to see. In summary, all future-pointing (past-pointing) null vectors at each point form the future (past) null cone of that point, but roughly half the vectors comprise an IN class, the other half forming an OUT class.

For the model one wishes to study here, the timelike radially infalling geodesics are the observers and emitters, whereas the (generally nonradial) null geodesics are the paths of photons through which these sources "see" one another. Because of the spherical symmetry, it is sufficient to study only equatorial $(\theta = \pi/2)$ trajectories to obtain the entire picture. Hence, the θ components of all subsequent vector quantities are suppressed.

To get the results for redshift behavior, one integrates the equations of motion for various geodesics in the Schwarzschild geometry to obtain, from the first integrals, the tangent vectors of the radial timelike sources and the tangent

vectors of the null paths which would connect them. Each radial observer or emitter has tangent vector:

$$\vec{U} = \left(\frac{dR}{dS}, 0, \frac{dT}{dS}\right) = \frac{1}{\sqrt{R}}\left(-1, 0, 1 + \frac{R}{1+\sqrt{R}}\right) \quad . \tag{6}$$

Each photon trajectory has tangent vector $\vec{K}_{\pm} = (\dot{R}, \dot{\phi}, \dot{T})$ expressed as one of

$$\vec{K}_{\pm} = \left(-\alpha, \beta R^{-2}, \frac{\alpha \pm R}{1 - R}\right) \quad , \tag{7}$$

where $(\pm)$ denotes the OUT or IN class, respectively. The parameter β is the angular momentum of the photon and is constant along any given photon trajectory. If $\beta = 0$, then it is a radial photon. The function α depends upon the coordinate R along any given photon trajectory but also depends upon the trajectory itself, through β:

$$\alpha(R, \beta) \equiv \left[1 + \left(\frac{\beta^2}{R^3}\right)(1 - R)\right]^{1/2} \quad .$$

The result [equation (7)] is valid for $\vec{K}_-$ throughout the space but is valid for $\vec{K}_+$ only inside the black hole, i.e., for $R < 1$.

Suppose an observer at R_0 receives a signal from an emitter which was at R_E. Then there is one more degree of freedom to be determined since R_E could lie anywhere on a circle; that degree of freedom is fixed by next choosing a value of β. Hence, the signal received by the fixed observer is characterized by a value for R_E and a value for β. However, the direction from which the observer receives the signal is only a function of β, i.e., the choice of photon trajectory going through R_0. If one follows a particular photon trajectory (β fixed) away from R_0, he runs over all possible R_E's that could have emitted that direction-dependent signal. It is the redshift seen by the observer that contains both the parameter β and the emitter position R_E. The correct redshift Z is contained in the formula:

$$1 + Z_{\pm} = \frac{f_{\pm}(R_E, \beta)}{f_{\pm}(R_0, \beta)} \quad , \tag{8}$$

where

$$f_{\pm}(R, \beta) \equiv \frac{\sqrt{R}}{1 - R} \left[\alpha(R, \beta) \pm \sqrt{R}\right] \quad .$$

Inside the black hole, β can run from 0 to ∞. We define $1 + Z_{\infty}$ = limit of $(1 + Z)$ as $\beta \to \infty$ so that

$$1 + Z_{\infty} = \frac{R_0 \sqrt{1 - R_0}}{R_E \sqrt{1 - R_E}} \tag{9}$$

completes equation (8) for all β.

By going to the local Lorentz frame of the observer (two dimensions of space, one of time), one can see the relationship of the direction parameter β "look angle" ω of the observer's celestial circle. The observer imagines the sum total of all directions he must look as being on a circle with him at the center. (This would be a sphere if we did not suppress the third dimension at the outset.) His local Lorentz frame is just a nonrotating set of two spatial directions and one time dimension (his clock). Suppose, without loss of generality, one of his spatial coordinate directions is the radially inward projection of the spacetime R-axis into his local frame. Then this direction could be called "ahead" of him and the opposite direction would be "behind" as he falls toward the center of the black hole; these are taken to be $\omega = 0$ and $\omega = 180°$, respectively. All $\vec{K}_+$ rays from $\beta = 0$ to $\beta = \infty$ then impinge on the observer at the angles ω_+: $0 \leq \omega_+ \leq \omega_\infty$, and the $\vec{K}_-$ rays from $\beta = 0$ to $\beta = \infty$ at the angles ω_-: $\omega_\infty \leq \omega_- \leq 180°$. The dependence of $\omega_\pm$ upon β is given by

$$\cos|\omega_\pm| = \frac{\sqrt{R_0} \cdot \alpha(R_0, \beta) \mp 1}{\alpha(R_0, \beta) \pm \sqrt{R_0}} \tag{10}$$

$$\cos|\omega_\infty| = \sqrt{R_0} \quad ,$$

ω_∞ giving the direction where the two ray classes interface on the null cone. These directions fill one half of his celestial circle; the celestial sphere would be constructed by rotating this circle about the diameter $\beta = 0$ with $\beta =$ constant $\neq 0$ corresponding to a whole ring of directions in the "sky" (Fig. 1).

The relationships in equations (8), (9), and (10) allow one to put together an analysis of possible redshifts and blueshifts in a given direction (β) by looking at ranges of values of R_E for each case. The picture is fixed by choosing at the outset a value for R_0 inside the black hole. Some details of this viewpoint are analyzed in Reference 3.

LUMINOSITY DISTANCE

Before any realistic evaluation of the redshift formulas in equations (8) and (9) can be made, it is necessary to answer the question: "What are the intensities of the redshifts in the various directions from the observer?" That is, if the rays from certain sources spread out too quickly, they may not be seen at all; therefore, the redshift is purely academic.

To solve this problem, one must tie luminosity distance to the redshift as various directions from the observer are investigated. Luminosity distance involves integrating along a single photon trajectory from emitter to observer so as to express the manner in which a small solid angle of rays at the emitter (pencil of rays) spreads and distorts on its way toward intercepting the observer. This is a complicated theoretical problem in nonlinear geometry and propagation of frames, but it is workable. Some of the preliminaries can be found in Reference 4. (No details leading to the results are to be given here but are postponed for a subsequent publication in collaboration with D. L. Farnsworth.)

For radial photons, the luminosity distance d is given by

$$d_\pm = (1 + Z)^{-1} \cdot \int_{R_0}^{R_E} \frac{\sqrt{R}}{1 \pm \sqrt{R}} \, dR \, , \tag{11}$$

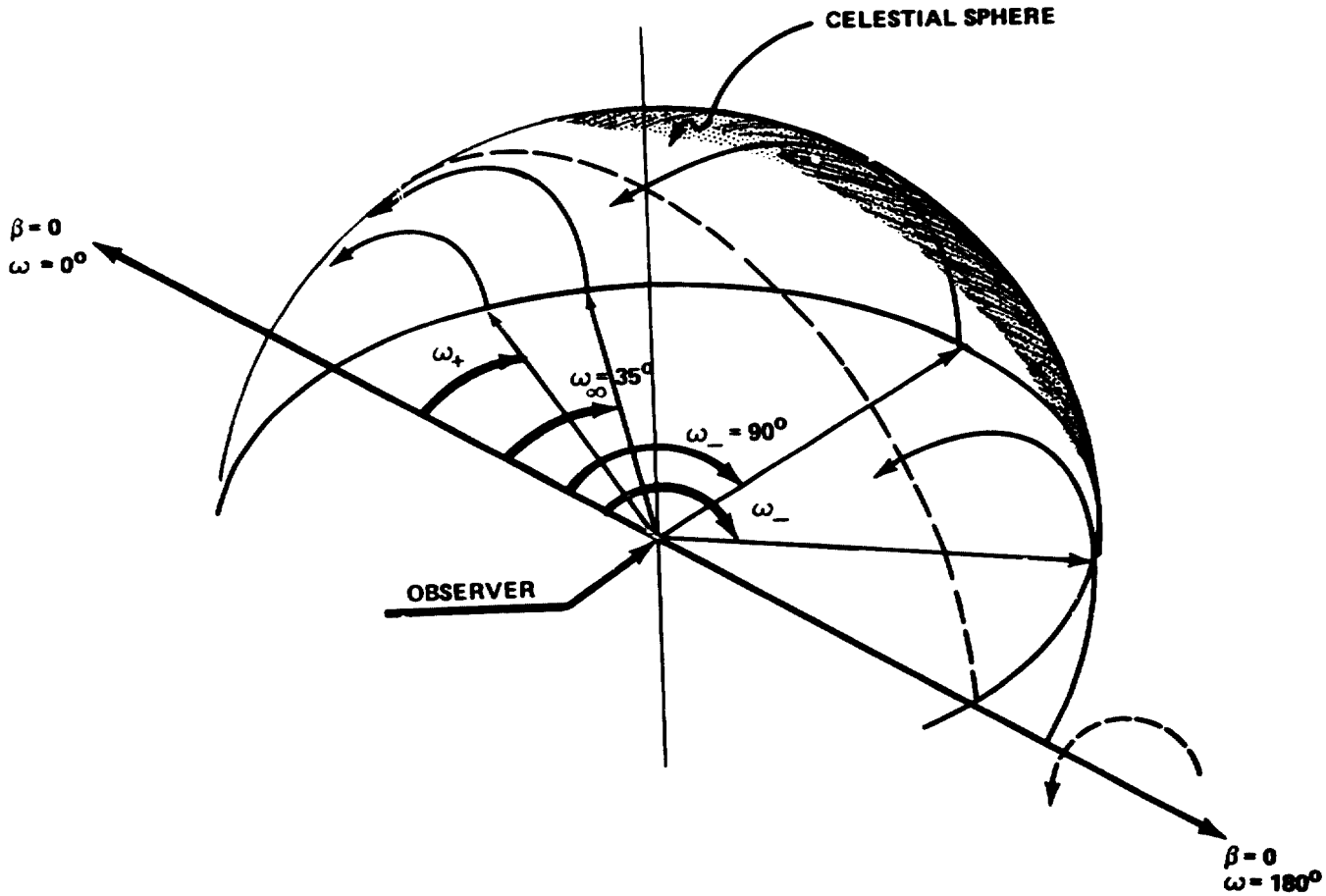

Figure 1. Observer's celestial sphere.

where (±) refers to the ray classes earlier, and $1 + Z$ is computed from equation (8) with $\beta = 0$.

For the $\beta = \infty$ case, the luminosity distance is found to be

$$d_\infty = (1 + Z_\infty)^{-1} \left[\frac{2R_0 \sin(\Delta\phi)}{\sqrt{1 - R_E}} \left(\sqrt{R_0} - \sqrt{R_E} + \tanh^{-1}\sqrt{R_E} - \tanh^{-1}\sqrt{R_0} \right) \right]^{1/2} , \tag{12}$$

where $\Delta\phi$ is the equatorial angle of travel of the photon:

$$\Delta\phi = \sin^{-1}(2R_E - 1) - \sin^{-1}(2R_0 - 1) \quad .$$

All other photon directions have an elliptic integral for the angle of travel $\Delta\phi$ [where "α" means simply $\alpha(R, \beta)$]:

$$\Delta\phi = \int_{R_0}^{R_E} \frac{\beta}{R^2 \cdot \alpha} \, dR \quad .$$

The luminosity distance in the two (±) cases is given through

$$(d_\pm)^2 = (1 + Z_\pm)^{-2} \frac{R_0 \sin(\Delta\phi)}{\sin\omega_E} \int_{R_0}^{R_E} \frac{\sqrt{R} \cdot (\alpha \pm \sqrt{R})}{\alpha \cdot (1 - R)} \, dR \quad , \tag{13}$$

where

$$\sin\omega_E \equiv \frac{1 - R_E}{\sqrt{R_E} \cdot R_E} \cdot \frac{\beta}{\alpha(R_E, \beta) \pm \sqrt{R_E}} \quad .$$

This is, again, an elliptic integral expression. For the study of these properties, a digital computer was utilized.

NUMERICAL RESULTS

The data may now be tabulated to make a proper comparison of redshift/blueshift anisotropy at various luminosity distances. The procedure is to choose first an observer (R_0). Next, a direction (β) of his celestial circle is fixed. By starting with values of R_E and going out in steps from $R_E \approx R_0$, one computes the redshift Z and luminosity distance d for an emitter at that value of R_E, as seen in that ω direction from the observer. The full equatorial coordinate values of the emitter are $R = R_E$ and $\phi = \Delta\phi$. This computation must be done twice, once for the $\vec{K}_-$ ray directions and once for the $\vec{K}_+$ ray directions.

Table 1 contains a summary of these data. The data are presented in steps of luminosity distance for greater ease of interpretation. Each set corresponds to a given "look angle" ω_- or ω_+, determined uniquely by β and received by the observer at $R_0 = 2/3$, $\phi = 0°$:

d_-, d_+ = luminosity distance of emitter at (R_E, $\Delta\phi$) in units of (r/2m) times 1000

Z_-, Z_+ = redshift/blueshift at the given d_-, d_+

$\Delta\phi$ = angular coordinate of emitter = azimuth angle of travel of photon (in degrees)

R_E = radial coordinate of emitter in units of (r/2m) times 1000.

DISCUSSION

Consider first the diagram depicted in Figure 2. The observer imagines "spheres" of constant radius about him, each of which corresponds to a certain "distance away." This latter distance is luminosity distance; therefore, an object he sees is placed on a sphere corresponding to that particular value of d in the particular direction ω from which it came to him. To this same object, there is a redshift Z assigned, and so forth, so that along any specified line of sight various redshifts occur. The intensity of these redshifts is completely

TABLE 1. REDSHIFT/BLUESHIFT DATA

d_-	Z_-	$\Delta\phi$	R_E	d_+	Z_+	$\Delta\phi$	R_E
($\beta = 0$)	$\omega_- = 180°$			$\omega_+ = 0°$			
101	0.083	0	900	9[illegible]	0.126	0	695
200	0.149	0	1140	194	0.231	0	715
300	0.204	0	1390	307	0.453	0	750
400	0.249	0	1640	398	0.747	0	785
480	0.281	0	1840	499	1.758	0	855
($\beta = 0.05$)	$\omega_- = 170°$			$\omega_+ = 1°$			
104	0.078	1.1	900	101	0.102	0.1	690
200	0.137	1.7	1120	200	0.211	0.3	714
303	0.190	2.2	1360	301	0.383	0.4	740
398	0.230	2.5	1580	408	0.609	0.6	770
502	0.269	2.8	1820	505	0.903	0.7	800
($\beta = 0.1$)	$\omega_- = 161°$			$\omega_+ = 2°$			
102	0.062	2.2	890	101	0.101	0.3	690
200	0.116	3.4	1110	200	0.225	0.6	714
302	0.163	4.3	1340	301	0.381	0.8	740
399	0.202	5.0	1560	408	0.607	1.1	770
465	0.226	5.1	1710	505	0.900	1.4	800
($\beta = 0.2$)	$\omega_- = 143°$			$\omega_+ = 4°$			
101	0.014	4.0	870	101	0.100	0.6	690
199	0.042	6.4	1070	200	0.222	1.1	714
302	0.075	8.[illegible]	1280	299	0.376	1.7	740
398	0.104	9.[illegible]	1480	407	0.599	2.3	770
499	0.132	10.5	1690	505	0.889	2.8	800
($\beta = 0.3$)	$\omega_- = 128°$			$\omega_+ = 6°$			
103	-0.041	5.4	850	100	0.098	0.8	690
199	-0.044	8.8	1020	200	0.219	1.6	715
300	-0.033	11.4	1200	299	0.367	2.5	740
400	-0.018	13.3	1380	406	0.586	3.3	770
499	0.00	14.8	1560	505	0.871	4.2	800

TABLE 1. (Continued)

d_-	Z_-	$\Delta\phi$	R_E	d_+	Z_+	$\Delta\phi$	R_E
(β = 0.5)	ω_- = 104°			ω_+ = 9°			
105	-0.119	7.0	810	100	0.093	1.3	691
199	-0.172	11.5	930	217	0.230	2.8	720
302	-0.203	15.3	1060	294	0.343	3.9	740
398	-0.218	18.1	1180	404	0.550	5.3	770
500	-0.226	20.6	1310	504	0.820	6.6	800
(β = 1.0)	ω_- = 73°			ω_+ = 16°			
100	-0.127	7.1	750	100	0.079	2.3	695
198	-0.212	12.5	820	205	0.181	4.6	720
305	-0.280	17.4	890	300	0.297	6.6	735
404	-0.329	21.3	950	393	0.441	8.6	770
471	-0.357	23.7	990	499	0.665	11.0	800
(β = 1.5)	ω_- = 60°			ω_+ = 20°			
97	-0.093	6.5	730	120	0.081	3.4	700
207	-0.170	12.4	790	194	0.142	5.4	720
300	-0.221	16.8	835	307	0.256	8.4	750
402	-0.269	21.1	880	400	0.375	11.0	775
500	-0.307	24.8	920	492	0.534	13.4	800
(β = 2.5)	ω_- = 49°			ω_+ = 25°			
103	-0.058	6.1	720	109	0.054	3.8	700
193	-0.096	10.8	760	215	0.120	7.3	730
295	-0.131	15.6	800	300	0.186	10.0	763
400	-0.160	20.1	836	400	0.283	13.2	780
506	-0.184	24.2	870	515	0.430	16.8	810
(β = 5.0)	ω_- = 42°			ω_+ = 30°			
98	-0.024	5.2	710	99	0.029	4.0	700
203	-0.040	10.3	750	196	0.068	7.7	730
292	-0.046	14.2	780	302	0.122	11.6	760
400	-0.049	19.0	815	414	0.196	15.5	790
496	-0.047	22.5	840	492	0.261	18.3	810

TABLE 1. (Concluded)

d_-	Z_-	$\Delta\phi$	R_E	d_+	Z_+	$\Delta\phi$	R_E
($\beta = 10.0$)	$\omega_- = 39°$			$\omega_+ = 32°$			
106	-0.009	5.3	710	100	0.018	4.4	702
200	-0.009	9.6	743	200	0.046	8.5	734
300	-0.002	13.8	775	300	0.083	12.3	764
[illegible]	0.011	17.9	804	396	0.128	15.9	790
497	0.030	21.6	830	513	0.201	20.2	820
($\beta = 25.0$)	$\omega_- = 36°$			$\omega_+ = 34°$			
111	0.0	5.4	710	100	0.011	4.6	704
199	0.008	9.2	740	210	0.033	9.2	740
296	0.023	13.2	770	311	0.062	13.2	770
401	0.048	17.4	800	400	0.096	16.6	794
500	0.079	21.2	826	499	0.143	20.3	820
$\beta = \infty$	$\omega_- = \omega_+ = 35°$						
100	0.005	4.7	705				
204	0.020	9.2	740				
303	0.042	13.2	770				
400	0.072	17.0	797				
500	0.112	20.8	823				

specified by the luminosity distance, and vice-versa. Redshifts (and blueshifts) at "large" (luminosity) distances are too weak to be seen, whereas those which are closer are seen more easily by the observer.

The data in Figure 2 are based on a standard unit of one black-hole radius for the scale of distance applied to values of d. The anisotropy of redshifts is clearly apparent. Towards the location of the center of the black hole ($\omega = 0°$), the observer sees the highest redshifts in his sky. There is a local clustering of redshifts in the diametrically opposite direction ($\omega = 180$), but these are not as great as the former. This axis ($\omega = 0°$ and $\omega = 180°$) forms the axis of symmetry about which the rest of the figure can be rotated to form the observer's celestial spheres of constant distance away.

No redshifts occur in the section of the sky corresponding to ω between 35° and 140°, and blueshifts achieve a maximum near the ring corresponding to $\omega = 73°$ in that region.

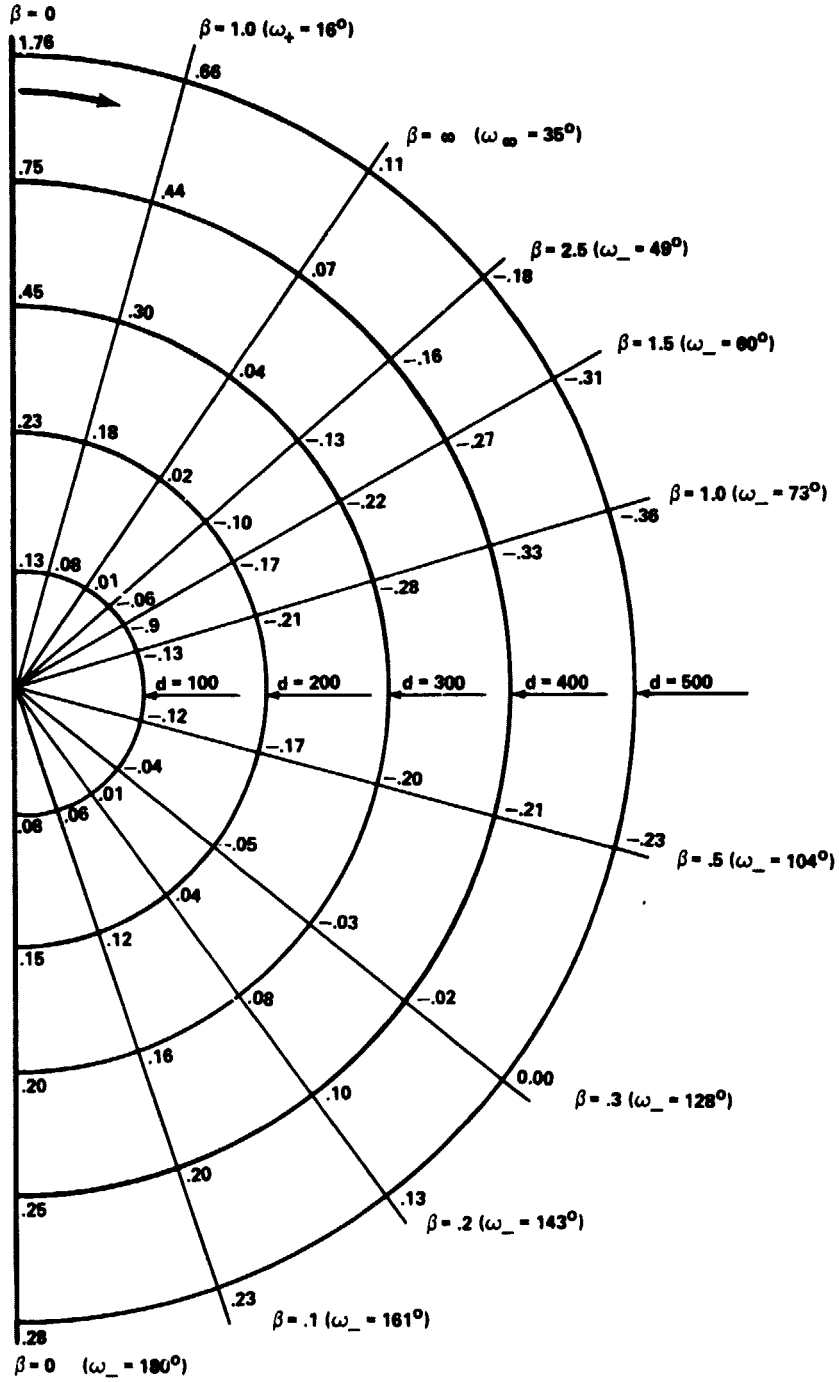

Figure 2. Red (blue) shifts at luminosity distance d.

AN EXOTIC APPLICATION: COSMOLOGICAL SCALING

Speculation about the universe as a black hole still has the status of folklore at this time, but this model is particularly adaptable to the examination of some of these ideas.

A spherical collapse of approximately one-tenth the mass of the universe at some early epoch would form a black hole whose horizon radius (= 2m) would be close to 10^{10} light years. The strength of the tidal forces within the horizon would then be near the normal forces experienced in a simple Friedmann model, at least in the region $m < r < 2m$. One does obtain a kind of cosmology with anisotropy if galaxies are the test particles. The time scale is quite large so that an observer needs to fall 10^9 years before appreciably changing his distance to the singularity at $r = 0$. His sky would contain a large number of redshifted objects, clustered about the two antipodal points of his celestial sphere ($\omega = 0°$ and $\omega = 180°$). A large ring of blueshifts would occur around $\omega = 73°$. Fennelly[1] interprets certain observational data on redshift anisotropy to point toward a maximum $\underline{Z}$ and minimum $\underline{Z}$ at two antipodal points of the sky.

The most obvious weakness here is the lack of mechanisms in this model to account for well-known isotropic phenomena, such as the microwave background and the distribution of QSO's. Also, work on the mass spectrum of primordial black holes [5] suggests that such a large black hole would be merely a fantastic coincidence.

1. Fennelly, A. J.: Private communication. To be published in Mon. Not. R. Astr. Soc., 1977.

REFERENCES

1. Carr, B. J., and Hawking, S. W.: Mon. Not. R. Astr. Soc., vol. 168, 1974, p. 399.

2. Hawking, S. W.: Comm. Math. Phys., vol. 43, 1975, p. 199.

3. Debney, G.: Mon. Not. R. Astr. Soc., vol. 176, September 1976, pp. 560-569.

4. Kristian, J., and Sacks, R. K.: Astrophysical J., vol. 143, 1966, pp. 379-399.

5. Carr, B. J.: Astrophysical J., vol. 201, 1975, pp. 1-19.

APPROVAL

TECHNIQUES OF GLOBAL ANALYSIS APPLIED TO GRAVITATION THEORIES: A COSMOLOGICAL BLACK HOLE?

By George Debney

The information in this report has been reviewed for security classification. Review of any information concerning Department of Defense or Atomic Energy Commission programs has been made by the MSFC Security Classification Officer. This report, in its entirety, has been determined to be unclassified.

This document has also been reviewed and approved for technical accuracy.

EUGENE W. URBAN
Chief, Cryogenic Physics Branch

RUDOLF DECHER
Chief, Space Physics Division

CHARLES A. LUNDQUIST
Director, Space Sciences Laboratory

☆U.S. GOVERNMENT PRINTING OFFICE 1977–740-049/236 REGION NO. 4